Out-of-plane and in-plane anisotropy of upper critical field in MgB_2

Z. X. Shi, M. Tokunaga, and T. Tamegai*
Department of Applied Physics, The University of Tokyo, 7-3-1 Hongo, Bunkyo-ku, Tokyo 113-8656, Japan

Y. Takano and K. Togano
National Institute for Materials Science, 1-2-1 Sengen, Tsukuba 305-0047, Japan
and Japan Science and Technology Corporation, 2-1-6 Sengen, Tsukuba 305-0047, Japan

H. Kito and H. Ihara
National Institute for Advanced Industrial Science and Technology, 1-1-1 Umezono, Tsukuba 305-8568, Japan
(Received 2 September 2002; revised manuscript received 6 January 2003; published 18 September 2003)

The anisotropy of the upper critical field in MgB_2 has been investigated on single crystalline, dense polycrystalline and powder samples by both transport and magnetic measurements. On the single-crystal sample, H_{c2}^{c} and H_{c2}^{ab} have been measured directly with applied field parallel to the *c* axis and *ab* plane. The angular dependence of H_{c2} shows deviation from the anisotropic Ginzburg-Landau model at lower temperatures. On polycrystalline and powder samples, H_{c2}^{c} and H_{c2}^{ab} have been determined by the method proposed by Bud'ko *et al.* The value of anisotropy parameter $\gamma=H_{c2}^{ab}/H_{c2}^{c}$ is temperature and sample dependent, and is about 3 and 4.5 for single and polycrystals, respectively, near T_c. However, $H_{c2}^{c}(T)$ are almost the same for all samples. These features could be an indication of anisotropic *s*-wave superconductivity with pancakelike energy gap or resulted from the different impurity levels in these samples. The anisotropy of H_{c2} in the *ab* plane has also been measured on single crystal and we set an upper bound of 1% for the in-plane anisotropy.

DOI: 10.1103/PhysRevB.68.104513 PACS number(s): 74.25.Fy, 74.25.Ha, 74.25.Op, 74.70.Ad

I. INTRODUCTION

MgB_2 has stimulated intense research activities all over the world for its highest T_c among intermetallic compounds and simple structure.[1] Its superconducting mechanism, two gap structure, anisotropic properties, and surface superconductivity are issues of recent interest. Among these issues, the anisotropy of the upper critical field is very important for both superconducting mechanism and applications of MgB_2. Is the newly found superconductor MgB_2 with layered structure two-dimensional (2D) superconductor like high-T_c superconductors or 3D superconductor like conventional low-T_c superconductors? After the discovery of this material, some experiments have been performed to estimate the anisotropy of upper critical field $\gamma=H_{c2}^{ab}/H_{c2}^{c}$. However, the value reported ranges between 1.1 and 13 and are dependent on samples and methods.[2] It is not very clear why γ depends on temperature and samples. It is also not clear whether the anisotropic behavior of MgB_2 obeys the anisotropic Ginzburg-Landau relation or not.

Generally, the anisotropy of one material can be estimated on single crystals, textured samples, epitaxial films, and aligned powders. Usually the anisotropy parameter is underestimated for aligned powders, epitaxial films, and textured samples due to the uncertainties in the degree of alignment or texture. Therefore the anisotropy parameter will be smaller than the real value, and the most reliable value is obtained for single crystals.

Since it is very difficult to prepare MgB_2 single crystals, only a few groups have synthesized MgB_2 single crystals at this point.[3–7] Before the preparation of single crystals, the anisotropy parameter is reported to be 1.1–1.7 for textured bulk and partially oriented crystallites,[8–10] 1.2 for *c*-axis oriented films,[11–13] and unexpectedly large values (5–9) for powders by the conduction electron-spin-resonance method.[14,15] After the preparation of single crystals, the anisotropy ratio has been determined to be 1.7–3 for single crystals by transport measurements[3–6] and to be 2–6 by magnetic measurements.[16–18] However, recently, Bud'ko *et al.*[14] proposed a different method to determine the anisotropy of the upper critical field on polycrystalline samples and powders and gave a values of $\gamma=6$. Even larger values of γ between 9 and 13 have been reported by Shinde *et al.*[19] for *c*-axis oriented films.

In this paper, we report our comparative studies on γ for single crystals and polycrystals by both transport and magnetic measurements. We also report in-plane anisotropy of H_{c2} by carefully aligning the magnetic field in the superconducting plane. This paper is organized as follows. Section I is an introduction. Section II describes the sample preparation methods and experimental techniques used in this paper, as well as the characterizations of our high quality MgB_2 single crystals. In Sec. III, results and discussions on the anisotropy in polycrystalline and single crystalline samples are presented. Section III A shows the upper critical fields and the anisotropy parameter determined on polycrystalline samples by the method from Ref. 14, and gives a detailed discussion of this method; Sec. III B is devoted to the accurate determination of the upper critical fields and the anisotropy parameter of single crystals. In Sec. III C the upper critical fields and the anisotropy parameter for different form of samples are compared. Section III D is specifically devoted to the angular dependence of the upper critical field both out of plane and in plane.

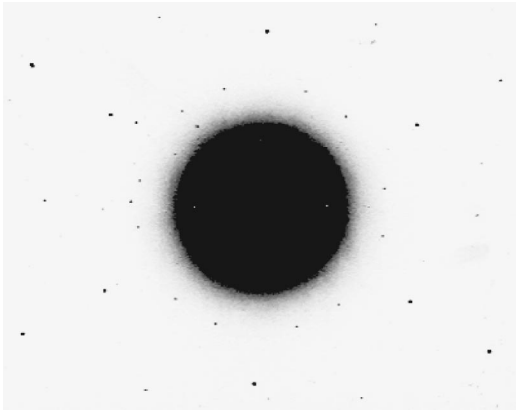

FIG. 1. Laue x-ray photograph of MgB_2 single crystal with x-ray parallel to the *c* axis.

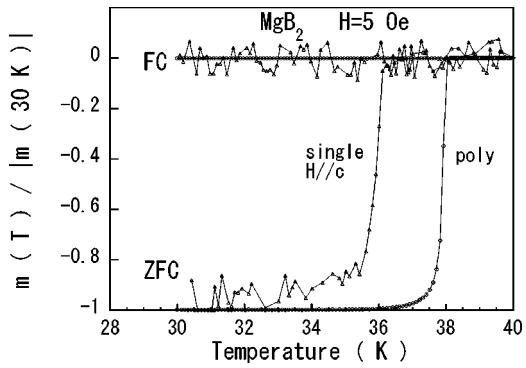

FIG. 2. Typical superconducting transitions at $H=5$ Oe for polycrystalline and single crystalline samples measured by SQUID magnetometer.

II. EXPERIMENT

Samples used in this paper are cylinders of pressed powders, dense polycrystalline samples, and single crystalline platelets. The MgB_2 powders and dense polycrystalline samples are prepared through directly reacting Mg and B in a Ta tube without pressure. Reaction of starting materials at 980° C for 1 h followed by quenching to room temperature produced powder samples of MgB_2, while dense polycrystalline samples were obtained by reacting Mg and B at 1400° C for 0.5 h, cooled down to 1000° C in 6 h, and then to room temperature in 2 h. The dense polycrystalline samples prepared in this way are porous. The x-ray diffraction reveals that these samples are pure with negligible impurity phase. For polycrystalline samples, no obvious defect has been found under the high-resolution polarizing microscopy and the superconducting critical temperatures (T_c's) are 38–39 K with transition width smaller than 0.2 K. For powder sample, T_c is about 38.5 K with larger ΔT_c.

The single crystalline samples are grown under a pressure of 3.5 GPa. The starting materials, $MgB_2+0.1$ Mg, were first heated to 1700° C in 25 min and kept for 30 min, then slowly cooled down to 1650° C in 6 h, and finally cooled rapidly down to room temperature. Its crystallinity has been checked by Laue x-ray photography. The peaks in the Laue photograph shown in Fig. 1 show a clear sixfold symmetry with negligible extra peaks, suggesting that the crystal is single domain. Though T_c's of single crystalline samples vary from piece to piece in the range of 36–38 K, the transition widths are smaller than 0.3 K. The single crystalline samples are thin platelets with thickness of about 20–50 μm. The typical superconducting transitions measured by superconducting quantum interference device (SQUID) magnetometer for polycrystalline and single crystalline samples are shown in Fig. 2

The upper critical field H_{c2} is determined by transport measurements using standard four-probe method and by magnetic measurements using SQUID magnetometer. For magnetic measurement, both zero-field-cooled (ZFC) and field-cooled (FC) magnetization curves are measured. For transport measurements of the anisotropy of H_{c2}, we use a two-axis sample rotator and a vector magnet system with maximum fields of 50 and 30 kOe for transverse and longitudinal directions, respectively. Both resistance vs temperature and resistance vs field curves are measured. In the in-plane anisotropy measurement, the field is aligned precisely parallel to the superconducting plane for each in-plane field direction.

III. RESULTS AND DISCUSSION

A. Powder and polycrystalline samples

Recently, Bud'ko *et al.*[14] proposed a method to determine the anisotropy of H_{c2} on polycrystalline and powder samples and reported an unexpectedly large value of $\gamma=6$. They determined the H_{c2}^c and H_{c2}^{ab} by characteristic features of the temperature derivative of magnetization $\partial M/\partial T$ at fixed field. Upon decreasing temperature there is an onset of diamagnetic signal and a sudden change of $\partial M/\partial T$ at T_c^{ab} due to the grain with the *ab* plane parallel to the applied field. With further decreasing temperature there is a peak of $\partial M/\partial T$ for the field-cold (FC) process and a kink of $\partial M/\partial T$ for the zero-field-cold (ZFC) process at T_c^c. Although it seems possible to determine the H_{c2}^{ab} and H_{c2}^c and obtain the information on the anisotropy parameter, there are several factors which affect the determination of H_{c2}^{ab} and H_{c2}^c by this method, especially the effect of flux pinning. Detailed discussions will be given as follows.

There are three factors influencing $\partial M/\partial T$ as well as the determination of H_{c2}^c. (i) The shielding current density and its radii, which increase with decreasing temperature and result in the increment of $\partial M/\partial T$ until H_{c2}^c. However, due to the distribution of T_c of grains at a fixed field resulted from the distribution of grain orientations, the maximum of $\partial M/\partial T$ may be a little higher than T_{c2}^c. (ii) The vortex-lattice melting, which causes the decrement of vortex density in sample and results in a sudden change in $\partial M/\partial T$, and affects the determination of H_{c2}^c. (iii) The flux pinning, which will prevent vortex coming in and out of the sample and affect the $\partial M/\partial T$ strongly. Depinning will also cause a sudden change in $\partial M/\partial T$ and affect the determination of H_{c2}^c. The influence of flux pinning on $\partial M/\partial T$ is different for FC and ZFC processes. In the FC process, flux pinning frus-

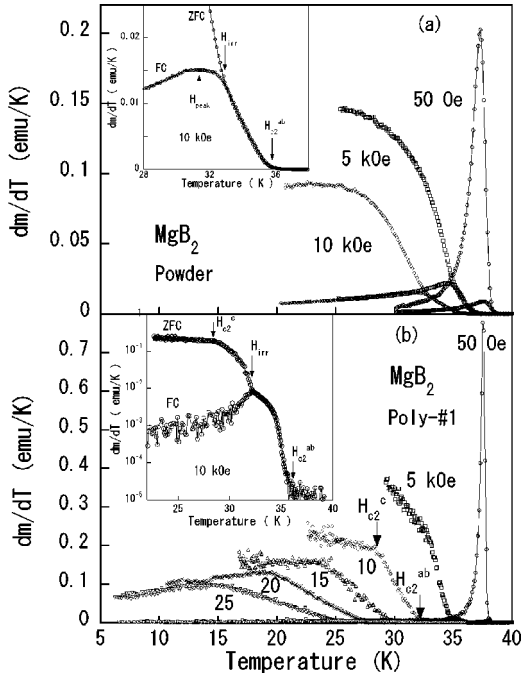

FIG. 3. Temperature dependence of the temperature derivative of magnetization $\partial M/\partial T$ in a fixed field for (a) powder (b) polycrystalline samples. The insets are the enlarged parts of FC process showing the determination of upper critical field and irreversibility field.

trates the vortex coming out of the sample and hinders the increment of the $\partial M/\partial T$, and the $\partial M/\partial T$ will reach its peak at a temperature higher than T_c^c, near the irreversibility point. So the anisotropy parameter will be underestimated by the peak of $\partial M/\partial T$ in the FC process. In the ZFC and warming process, flux pinning prevents the entry of vortex into the sample and at lower temperatures the $\partial M/\partial T$ is mainly contributed from $\partial J_c/\partial T$, the change of critical current density with temperature. The rapid change of $\partial J_c/\partial T$ at temperatures lower than T_c^c (near T_c^c) will move the kink of $\partial M/\partial T$ in the ZFC process to temperatures lower than T_c^c. So the anisotropy of the upper critical field may be overestimated by the kink of $\partial M/\partial T$ in the ZFC and warming process. The real T_c^c should be between the peak of $\partial M/\partial T$ in the FC process and the kink of $\partial M/\partial T$ in the ZFC process. So this method can give the upper and lower bounds for H_{c2}^c and anisotropy parameters.

Of course, if the sample is inhomogeneous, the kink of $\partial M/\partial T$ in the ZFC process and the peak of $\partial M/\partial T$ in the FC process will be smeared due to the span of T_c and it will be very difficult to determine real T_c^c. So it is better to estimate the anisotropy parameter of H_{c2} by this method on homogeneous samples with weak flux pinning.

To test our analysis, we have measured the magnetizations in both the ZFC and FC processes at fixed fields in a wide temperature range on powder-pressed cylinder and polycrystalline samples, and the temperature dependence of $\partial M/\partial T$ has been derived. The typical data are shown in Figs. 3(a) and (b). The kinks of $\partial M/\partial T$ in the ZFC process corresponding to T_c^c are more clear for the polycrystalline sample than

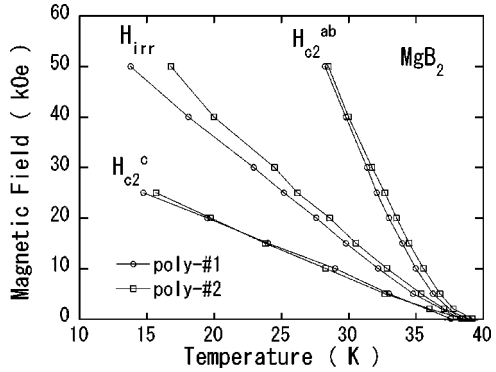

FIG. 4. Temperature dependence of upper critical field H_{c2}^c and H_{c2}^{ab} and irreversibility field H_{irr} for two polycrystalline samples. H_{c2}^c and H_{c2}^{ab} are determined by the kink and onset points in ZFC. H_{irr} is determined by the separating point of $\partial M/\partial T$ in ZFC and FC processes.

for the powder sample due to the span of T_c in the powder sample. And the peak in FC is also broadened for the powder sample as shown in the inset of Fig. 3(a). For the polycrystalline sample, the peak of $\partial M/\partial T$ in the FC process is almost the same as the irreversibility point, the separating point of FC and ZFC, due to the effect of flux pinning as shown in the inset of Fig. 3(b). And the temperature of the peak of $\partial M/\partial T$ in FC is much higher than the temperature of kink in ZFC due to the effect of flux pinning. This is quite different from the results in Ref. 14, where the peak in FC and the kink in ZFC are at almost the same temperature. For MgB_2, the critical current density changes linearly with temperature[20] and the relative influence on $\partial M/\partial T$ is gradual and smaller compared with the sudden change of the shielding current density and its radii at T_c^c, which may result in the kink of $\partial M/\partial T$. So it seems better to deduce the H_{c2}^c from the ZFC process data. The temperature dependences of upper critical fields H_{c2}^c and H_{c2}^{ab} and the irreversibility field H_{irr} are shown in Fig. 4 for two polycrystalline samples. To give a bound to anisotropy parameters, the anisotropy parameters are calculated by using the data of H_{c2}^c from both the FC (H_{irr}) and ZFC (H_{c2}^c) processes. Temperature dependences of γ for both processes are shown in Fig. 5.

B. Single crystalline samples

Though the method proposed by Bud'ko can be used for rough estimation of the anisotropic H_{c2} of MgB_2, it is necessary to study single crystalline samples to determine the anisotropy of H_{c2} accurately. Figures 6(a) and (b) show the temperature dependence of resistance $R(T)$ curves at several fields both for $H//c$ axis and $H//ab$ plane. It is obvious that the upper critical field and the irreversibility field are quite different for the two configurations and superconductivity in MgB_2 is anisotropic. However, it is not easy to determine the accurate values of H_{c2} due to the significant broadening of the transition. The $R(T)$ curve exhibits a kink structure for both field directions though the broadening of transition is suppressed for $H//ab$ plane. The structure of $R(T)$ curves shows a strong dependence on transport current density and

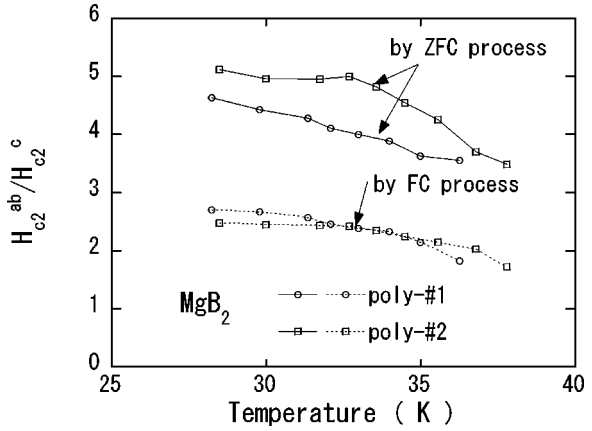

FIG. 5. Temperature dependence of anisotropy parameter calculated by using the data of H_{c2}^{c} deduced from both the FC (H_{irr}) and ZFC (H_{c2}^{c}) processes.

non-Ohmic behavior for both field directions, as shown in the inset of Fig. 6(b). These unusual and remarkable features are consistent with the previous reports and could be explained by two-gap model or surface superconductivity.[16,21]

For the investigation of the origin of the transition broadening in MgB_2, direct magnetic measurements have also been performed on the same single crystalline sample. Figures 7(a) and (b) show the temperature dependence of FC and ZFC magnetization of the single crystal for $H//c$ axis and *ab* plane, respectively. Both H_{c2}^{ab} and H_{c2}^{c} are determined by the onset of diamagnetism, as shown in the inset of Fig. 7(b). This graph also shows the anisotropy of the upper critical field in MgB_2. Because the sample is small and hence the signal is small on top of large background noise, we cannot measure it at higher fields. However, no kinks are found in the magnetization curves, which is quite different from the $R(T)$ curves. The onset of diamagnetism closely follows the line of H_{c2} determined by the peak of $\partial R/\partial T$. This fact strongly suggests that the kink structure is not a sign of bulk superconductivity but originated from surface superconductivity. Due to the effect of surface superconductivity, we propose to take the onset of resistive transition as H_{c3}, and the kink point or the sharpest point of $R(T)$ curves (the peak of $\partial R/\partial T$ curves) as real H_{c2}. The temperature dependence of upper critical field determined in this way is shown in Fig. 8.

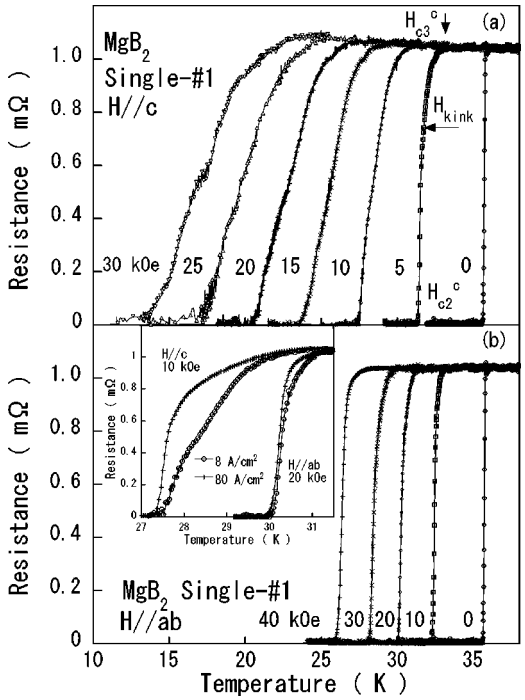

FIG. 6. Temperature dependence of in-plane resistance $R(T)$ at several fields for (a) $H//c$ axis and (b) $H//ab$ plane. The inset shows the current density dependence of resistance for both $H//c$ axis and $H//ab$ plane.

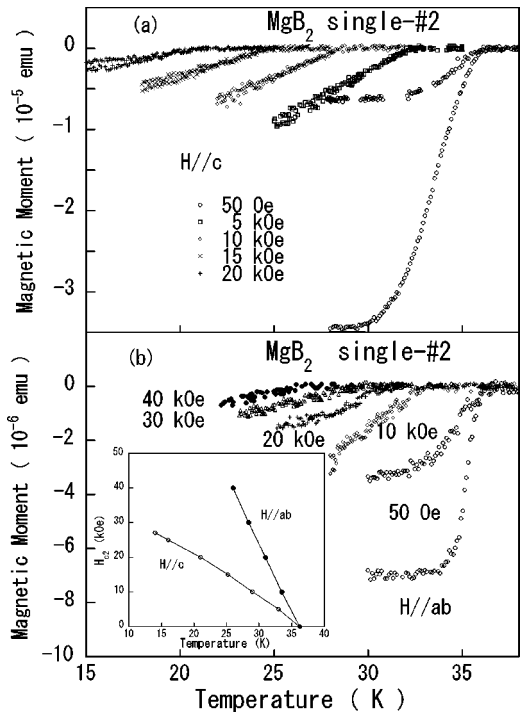

FIG. 7. Temperature-dependent ZFC and FC magnetization curves at several fields for (a) $H//c$ and (b) $H//ab$. The inset shows the upper critical fields determined by the start point of transition.

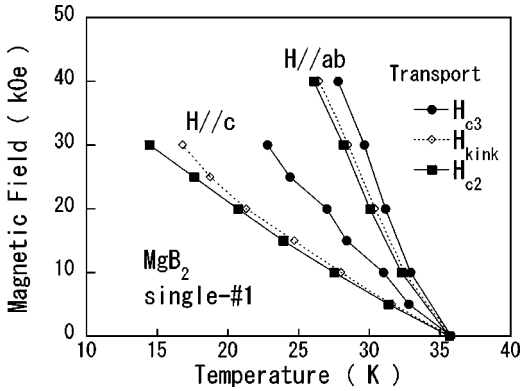

FIG. 8. Temperature dependence of the upper critical fields deduced from the $R-T$ curves. H_{c3} and H_{kink} are defined as the onset point and the kink point, H_{c2} is determined by the peak of $\partial R/\partial T$ curves.

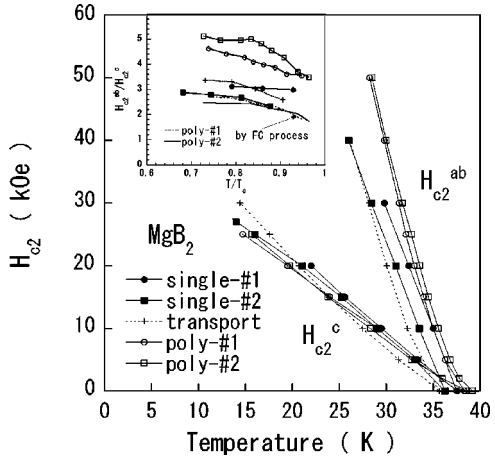

FIG. 9. Temperature dependence of the upper critical fields H_{c2}^{c} and H_{c2}^{ab} deduced from the $R-T$ and $M-T$ curves for both single crystalline and polycrystalline samples. The inset shows the temperature dependence of anisotropy parameter $\gamma=H_{c2}^{ab}/H_{c2}^{c}$ of these samples.

H_{c3}^{c} is 1.64 times larger than H_{c2}^{c} and H_{c3}^{ab} is 1.32 times larger than H_{c2}^{ab} in contrast to the theoretical value of $H_{c3}=1.695H_{c2}$.[22] So this is another direct evidence of surface superconductivity.

C. Comparison of H_{c2} in polycrystalline and single crystalline samples

From the above data, the temperature dependence of H_{c2}^{ab} and H_{c2}^{c} can be compared for polycrystalline and single crystalline samples, as shown in Fig. 9. The inset of Fig. 9 shows the temperature dependence of the anisotropy parameter $\gamma=H_{c2}^{ab}/H_{c2}^{c}$. H_{c2}^{ab} and H_{c2}^{c} have different temperature dependence and hence γ is also temperature dependent, which implies a breakdown of the anisotropy of the band effective mass or may be related to the anisotropy of the energy-gap structure of MgB_2. γ is sample dependent and is about 2.5 for single crystalline samples and 4 for polycrystalline samples at temperatures near T_c, which may be resulted from the overestimation by the ZFC data for polycrystalline samples. The values of γ for single crystals are between the upper and lower bounds set by polycrystalline samples. However, H_{c2}^{ab} is obviously sample dependent while H_{c2}^{c} is almost independent of samples. These features may be resulted from two origins: (i) The pancakelike energy gap anisotropy proposed by Posazhennikova *et al.*,[23] which may result in a larger change of H_{c2}^{ab} while a smaller change of H_{c2}^{c} for samples with different γ values and can result in temperature-dependent γ. (ii) Different impurity levels, which can also result in this phenomenon because H_{c2}^{c} only depends on ξ_{ab}, $H_{c2}^{c}(0)=\Phi_0/(2\pi\xi_{ab}^2)$, while H_{c2}^{ab} depends on both ξ_{ab} and ξ_c, $H_{c2}^{ab}(0)=\Phi_0/(2\pi\xi_{ab}\xi_c)$. So if only ξ_c is different for different samples, H_{c2}^{ab} and γ will change and H_{c2}^{c} will not change for samples with different impurity levels.

As shown in Fig. 9, H_{c2}^{c} follows a conventional temperature dependence and $H_{c2}^{c}(0)$ is estimated to be about 35.1 kOe using $H_{c2}(0)=0.73T_c[-dH_{c2}(T)/dT]$,[24] with average slope $dH_{c2}^{c}(T)/dT=-0.13$ T/K and $T_c=37$ K. By $H_{c2}^{c}=\Phi_0/(2\pi\xi_{ab}^2)$, $\xi_{ab}(0)$ is about 9.5 nm. By simple extrapolation of H_{c2}^{ab} lines to zero-temperature axis, $H_{c2}^{ab}(0)$ ranges from 141 to 191 kOe, and $\xi_c(0)$ ranges from 1.76 to 2.4 nm. So the value of γ should be smaller than 5.5 at zero temperature.

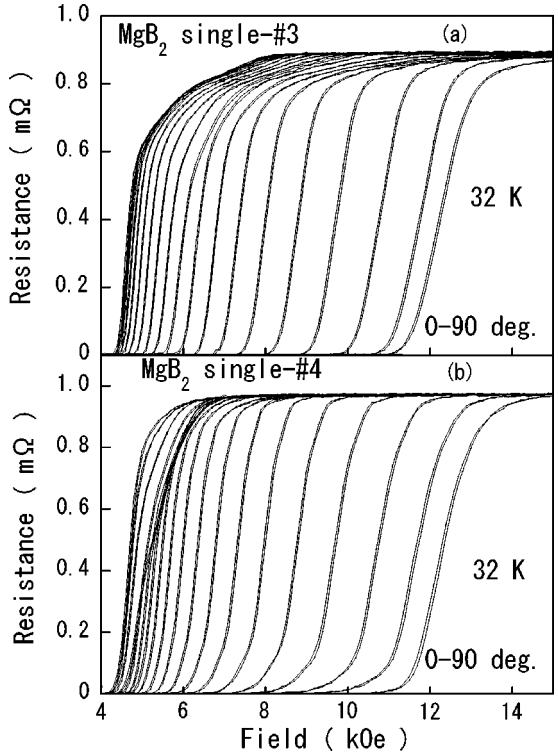

FIG. 10. Field dependence of in-plane resistance at 32 K of two single-crystal samples with the field applied at different angles from the c axis between 0° and 90° every 5°.

D. Angular dependence of H_{c2}

For more accurate determination of anisotropy of H_{c2}, the $R-H$ curves have been measured at different angles θ and different temperatures on two single crystals, as shown in Figs. 10(a) and (b). Here θ is the angle of the field from the c axis. The shape of the transition curves changes with the angle θ due to the anisotropy of surface superconductivity. Fine structures of the transition curves for the two samples are different because of their different shapes. Sample 4 is about twice as thick as sample 3. At zero field the T_c of sample 4 is about 1 K lower than the T_c of sample 3. To avoid effects of surface superconductivity and inhomogeneties, we define H_{c2} at each θ as the peak of $\partial R/\partial H$. The values of upper critical field $H_{c2}(\theta)$ determined in this way are almost the same for the two samples, as shown in Figs. 11(a) and (b). The angular dependence is distorted if the midpoint of transition is taken as the H_{c2}. It is obvious that there is no universality of Ginzburg-Landau (GL) relation with an effective mass anisotropy in MgB_2 and the anisotropy parameter γ is temperature dependent. The inset of Fig. 11(b) shows the temperature dependence of γ determined by

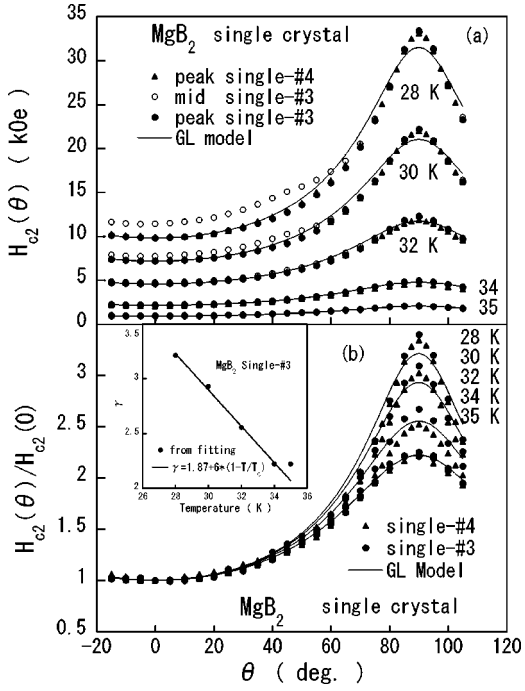

FIG. 11. (a) Angular dependence of H_{c2} for MgB_2 single crystals 3 and 4 deduced from Fig. 10, the peak of $\partial R/\partial H$ curves and the mid point of $R-H$ curves. (b) Angular dependence of normalized H_{c2}. Solid lines are fit by the anisotropic GL model and inset shows the temperature dependence of anisotropy parameter determined by best fitting.

the best fitting with anisotropic GL model, $H_{c2}(\theta) = H_{c2}(0)(\cos^2\theta + \sin^2\theta/\gamma^2)^{-0.5}$. At temperatures near T_c, the $H_{c2}(\theta)$ can be reasonably well fitted by anisotropic GL relation, while at lower temperatures, it deviates from the GL model. The peak at 90° is sharper than the GL model, which may be resulted from the effect of special energy gap structure of MgB_2 or just the effect of surface superconductivity on the determination of H_{c2}. To sort out the origin of the deviation from the GL model, angular dependence of bulk qualities such as magnetization and specific heat is necessary. The value of γ near T_c is about 2.2, which may be the real parameter of effective-mass anisotropy. The temperature dependence of γ can be fitted with relation $\gamma(T) = \gamma^* + k(1-T/T_c)$. Here $\gamma^* = 1.87$ is the band effective mass anisotropy and $k=6$ may be resulted from the anisotropy of attractive electron-electron interaction. This result is very similar to that reported by Angst *et al.*[17]

Using the same method, we also measured the in-plane anisotropy of the upper critical field $H_{c2}(\phi)$ by carefully aligning the magnetic field exactly in the *ab* plane for each ϕ within 0.01°. The current is passed along the *a* axis, where we define the direction of the in-plane field $\phi = 0°$. Figure 12 shows $H_{c2}(\phi)$ at $T=32$ K for two samples measured with two different current densities. As is evident from the

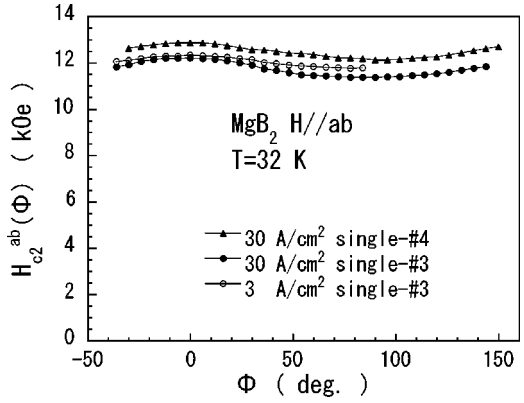

FIG. 12. Angular dependence of upper critical field in the *ab* plane, $H_{c2}^{ab}(\phi)$, for two single crystalline samples and the current density dependence of $H_{c2}^{ab}(\phi)$.

figure, the dominant component of $H_{c2}(\phi)$ has a twofold symmetry rather than the sixfold symmetry expected from the hexagonal crystal structure. The twofold symmetry is due to the Lorentz force as evidenced by the current density dependence and the minimum of $H_{c2}(\phi)$ for a field perpendicular to the current. After subtracting the twofold symmetry component, the sixfold symmetry component is less than 1%. This result is consistent with the prediction that the sixfold symmetry part of H_{c2} is absent in hexagonal systems.[25] However, it should be noted that a clear anisotropy of $H_{c2}(\phi)$ more than 30% in hexagonal material Cs_xWO_3 is reported in high quality single crystals.[26]

In conclusion, we have studied the anisotropy of H_{c2} on powder, polycrystalline, and single crystalline samples comparatively by both magnetic and transport measurements. Angle-resolved magnetotransport properties have also been studied on single crystals in the *ab* plane and out of plane. The out-of-plane anisotropy deviates from the GL model at lower temperatures, and temperature dependence of γ implies a breakdown of the GL model with an effective-mass anisotropy, which may be resulted from the special energy gap structure in MgB_2. The sample dependence of γ could be an indication of anisotropic *s*-wave superconductivity with pancakelike energy gap or resulted from the different impurity levels in these samples, or just due to the overestimation of γ for polycrystalline samples by the method proposed by Bud'ko. Though this method is not very accurate, the anisotropy parameter could be estimated roughly, especially on homogeneous polycrystalline samples with weak flux pinning. There is almost no anisotropy in the *ab* plane.

ACKNOWLEDGMENT

This work was partly supported by a Grant-in-Aid for Scientific Research from the Ministry of Education, Science, Sports and Culture, Japan.

*Author to whom correspondence should be addressed. Electronic address: tamegai@ap.t.u-tokyo.ac.jp
[1] J. Nagamatsu, N. Nakagawa, T. Muranaka, Y. Zenitani, and J. Akimitsu, Nature (London) **410**, 63 (2001).
[2] C. Buzea and T. Yamashita, Supercond. Sci. Technol. **14**, R115-R146 (2001).
[3] M. Xu, H. Kitazawa, Y. Takano, J. Ye, K. Nishida, H. Abe, A. Matsushita, and G. Kido, Appl. Phys. Lett. **79**, 2779 (2001).
[4] K.H.P. Kim, J.-H. Choi, C.U. Jung, P. Chowdhury, H.-S. Lee, M.-S. Park, H.-J. Kim, J.Y. Kim, Z. Du, E.M. Choi, M.-S. Kim, W.N. Kang, S.-Ik. Lee, G.Y. Sung, and J.Y. Lee, Phys. Rev. B **65**, 100510(R) (2002).
[5] Sergey Lee, Hatsumi Mori, Takahiko Masui, Yuri Eltsev, Ayako Yamamoto, and Setsuko Tajima, J. Phys. Soc. Jpn. **70**, 2255 (2001).
[6] A.K. Pradhan, Z.X. Shi, M. Tokunaga, T. Tamegai, Y. Takano, K. Togano, H. Kito, and H. Ihara, Phys. Rev. B **64**, 212509 (2001).
[7] J. Karpinski, M. Angst, J. Jun, S.M. Kazakov, R. Puzniak, A. Wisniewski, J. Roos, H. Keller, A. Perucchi, L. Degiorgi, M. Eskildsen, P. Bordet, L. Vinnikov, and A. Mironov, Supercond. Sci. Technol. **16**, 221 (2003).
[8] A. Handstein, D. Hinz, G. Fuchs, K.-H. Muller, K. Nenkov, O. Gutfleisch, V.N. Narozhnyi, and L. Schultz, J. Alloys Compd. **329**, 285 (2001).
[9] O.F. de Lima, R.A. Ribeiro, M.A. Avila, C.A. Cardoso, and A.A. Coelho, Phys. Rev. Lett. **86**, 5974 (2001).
[10] O.F. de Lima, C.A. Cardoso, R.A. Ribeiro, M.A. Avila, and A.A. Coelho, Phys. Rev. B **64**, 144517 (2001).
[11] M.H. Jung, M. Jaime, A.H. Lacerda, G.S. Boebinger, W.N. Kang, H.J. Kim, E.M. Choi, and S.I. Lee, Chem. Phys. Lett. **343**, 447 (2001).
[12] C. Ferdeghini, V. Ferrando, G. Grassano, W. Ramadan, E. Bellingeri, V. Braccini, D. Marre, P. Manfrinetti, A. Palenzona, F. Borgatti, R. Felici, and T.-L. Lee, Physica C **378**, 56 (2002).
[13] S. Patnaik, L.D. Cooley, A. Gurevich, A.A. Polyanskii, J. Jiang, X.Y. Cai, A.A. Squitieri, M.T. Naus, M.K. Lee, J.H. Choi, L. Belenky, S.D. Bu, J. Letteri, X. Song, D.G. Schlom, S.E. Babcock, C.B. Eom, E.E. Hellstrom, and D.C. Larbalestier, Supercond. Sci. Technol. **14**, 315 (2001).
[14] S.L. Bud'ko, V.G. Kogan, and P.C. Canfield, Phys. Rev. B **64**, 180506(R) (2001).
[15] F. Simon, A. Janossy, T. Feher, F. Muranyi, S. Garaj, L. Forro, C. Petrovic, S.L. Bud'ko, G. Lapertot, V.G. Kogan, and P.C. Canfield, Phys. Rev. Lett. **87**, 047002 (2001).
[16] A.K. Pradhan, M. Tokunaga, Z.X. Shi, Y. Takano, K. Togano, H. Kito, H. Ihara, and T. Tamegai, Phys. Rev. B **65**, 144513 (2002).
[17] M. Angst, R. Puzniak, A. Wisniewski, J. Jun, S.M. Kazakov, J. Karpinski, J. Roos, and H. Keller, Phys. Rev. Lett. **88**, 167004 (2002).
[18] Ken'ichi Takahashi, Toshiyuki Atsumi, Nariaki Yamamoto, Mingxiang Xu, Hideaki Kitazawa, and Takekazu Ishida, Phys. Rev. B **66**, 012501 (2002).
[19] S.R. Shinde, S.B. Ogale, A. Biswas, R.L. Greene, and T. Venkatesan, cond-mat/0110541 (unpublished).
[20] Z.X. Shi, M. Tokunaga, A.K. Pradhan, T. Tamegai, Y. Takano, K. Togano, H. Kito, and H. Ihara, Physica C **370**, 6 (2002).
[21] U. Welp, G. Karapetrov, W.K. Kwok, G.W. Crabtree, Ch. Marcenat, L. Paulius, T. Klein, J. Marcus, K.H.P. Kim, C.U. Jung, H.-S. Lee, B. Kang, and S.-I. Lee, Phys. Rev. B **67**, 012505 (2003).
[22] D. Saint-James and P.G. de Gennes, Phys. Lett. **7**, 306 (1963).
[23] A.I. Posazhennikova, T. Dahm, and K. Maki, Europhys. Lett. **60**, 134 (2002).
[24] S. Haas and K. Maki, Phys. Rev. B **65**, 020502 (2001).
[25] L.I. Burlachkov, Sov. Phys. JETP **62**, 800 (1985).
[26] M.R. Skokan, W.G. Moulton, and R.C. Morris, Phys. Rev. B **20**, 3670 (1979).